

Harsh-Environmental-Resistant Triboelectric Nanogenerator and Its Applications in Autodrive Safety Warning

Jing Wen, Baodong Chen, Wei Tang, Tao Jiang, Laipan Zhu, Liang Xu, Jian Chen, Jiajia Shao, Kai Han, Wen Ma,* and Zhong Lin Wang*

Rapid advancements in multifunctional triboelectric nanogenerators (TENGs) for energy harvesting and self-powered sensing must be partnered with corresponding advances in durability and heat-resistance, especially under harsh working conditions. A device suitable for harsh environmental applications based on the wear-resistant triboelectric material is reported. The working modes of the harsh-environmental TENG (heTENG) are composed of freestanding and single electrode that enable both harvesting sliding/vibration energy and self-powered vibrational sensing. For the first time, a TENG possessing wear resistance, withstanding high temperature, and high hardness is achieved by employing micro–nanocomposite for triboelectric materials. It is demonstrated to be directly used as a key supporting part, such as automobile's brake pads. In addition, it is found that the heTENG outputs 221 V, 27.9 $\mu\text{A cm}^{-2}$, and 33.4 $\mu\text{C cm}^{-2}$. Furthermore, since heTENG is vibration-sensitive, the automobile's self-powered smart braking system and sensor network are developed successfully which can automatically provide a precise early-warning signals, such as a reminder for brake replacement, and an indicator for tire overloading, and pressure. This work shows a new strategy to enhance the performance of triboelectric materials, making it applicable to harsh environments, as well as potential applications in autonomous vehicles and industrial brakes.

ambient energy. TENG is of great interest for capturing low-frequency mechanical energy due to its low cost in fabrication and excellent coupling effect (triboelectric effect and electrostatic induction). Different structures and triboelectric materials of triboelectric nanogenerators (TENGs) have been designed for harvesting mechanical energy of different form, e.g., water wave, wind, vibration, and biomechanical motion energy from the natural environment.^[6–12]

Recently, based on the artificial intelligence (AI) technology, autonomous car (driverless, self-driving, robotic) is an innovative vehicle that is capable of sensing its environment and navigating without human input. Driving safety early warning (DSEW) system is very important for in the cruising of autonomous vehicles, and it is a key technology that has been proposed and developing fast in this field. In fact, information cannot be provided without a strong efficient sensor network. TENGs could be harvesting vibrational/slide energy from a moving

vehicle, as power sources and self-powered sensors for DSEW system.^[13–15] However, there are some limitations to the previously different kinds of TENGs. First, the triboelectric materials' supporting surface is easy to be damaged during the contact and the separation, it is unable to support sliding friction for long periods. Second, most organic triboelectric materials

1. Introduction

Triboelectric nanogenerator (TENG) as a newly invented energy harvesting technology that can effectively converting arbitrary mechanical energy into electricity has been extensively investigated,^[1–5] aiming at harnessing much underutilized the

J. Wen, Dr. B. Chen, Prof. W. Ma
School of Materials Science and Engineering
Inner Mongolia University of Technology
Inner Mongolia Key Laboratory of Thin Film and Coatings Technology
Hohhot 010051, China
E-mail: wma@imut.edu.cn

J. Wen, Dr. B. Chen, Dr. W. Tang, Dr. T. Jiang, Dr. L. Zhu, Dr. L. Xu,
J. Chen, J. Shao, K. Han, Prof. Z. L. Wang
Beijing Institute of Nanoenergy and Nanosystems
Chinese Academy of Sciences
Beijing 100083, China
E-mail: zhong.wang@mse.gatech.edu

 The ORCID identification number(s) for the author(s) of this article can be found under <https://doi.org/10.1002/aenm.201801898>.

Dr. B. Chen, Dr. W. Tang, Dr. T. Jiang, Dr. L. Zhu, Dr. L. Xu, J. Chen,
J. Shao, K. Han, Prof. Z. L. Wang
CAS Center for Excellence in Nanoscience
National Center for Nanoscience and Technology (NCNST)
Beijing 100190, China
Prof. Z. L. Wang
School of Material Science and Engineering
Georgia Institute of Technology
Atlanta, GA 30332, USA

DOI: 10.1002/aenm.201801898

can be a considerably decompose or deformation significantly when the operating temperature is higher than 200 °C. Thus, TENGs are primarily used as additional components rather than the key supporting parts and limit their applications in industrial sectors. Therefore, with the wear resistance and withstand high temperatures performance are required for TENG's triboelectric materials. To breakthrough these limitations, previous research has shown that mainly by use of the excellently macromolecule polymer materials like polytetrafluoroethylene (PTFE), polyimides, and special compound modification.^[16–20] Besides, a lot of the unique structure's TENGs have also been reported, which are based on the structure optimization and protective packaging of the TENGs.^[12,21–25]

In this article, we design an enough to deal with the harsh-environmental TENG (heTENG), demonstrate a new wear-resistant triboelectric material by hybridizing micro–nanocomposite as triboelectric layer that is directly used for key wear-resistant parts. Based on the excellent wear resistance and withstand high temperatures, the sliding/vibration energy harvesting and self-powered sensing are achieved in harsh working environment. For instance, the heTENG was integrated with the braking system of vehicle, as a self-powered smart braking (SP-SB) device which can alert the replacement of brake pads. Additionally, whereas it is vibration-sensitive, a novel type of vibrational SP-SB sensor network is constructed for safety monitoring of vehicle with combinations of four heTENGs, such as tire pressure, overloading, and partly load. The integrated SP-SB in a vehicle can not only acquire vibrational signal of the driving status but also supply the DSEW and take proper action in real time. Eventually, we hope that the heTENG will be able to sense just about anything vibration with disadvantageous to the running safety of vehicles, offering a tantalizing vision of applications such as autonomous vehicles.

2. Results and Discussion

The wear-resistant triboelectric materials were prepared by hybridizing micro–nanocomposite. Its morphology and microstructure were shown in **Figure 1**. Figure S1 of the Supporting Information shows the fabrication process in detail. The results show that the composite possesses fine and uniform microstructure and excellent wear resistance in which slide and abrasive wear are dominant in the wear behavior (Figure 1b–d). The thermal diffusivity and hot weightlessness rate show that the material has great thermal stability. When the composites were heated in temperature range of 25 to 550 °C, making it possible to withstand the larger friction and creating heat with the friction (Figure 1e,f). The results showed that the micro–nanocomposite had a good wear resistance that the mean dynamic friction coefficient of $\approx 0.69 \mu\text{m}$ at low-friction of about 8.1 N and room temperature (Figure 1d; Figure S1e, Supporting Information), and it had excellent high-temperature tolerance (temperature ring of -30 to 550 °C), the wear-resisting ability (Figure S1f, Supporting Information), and high hardness (Rockwell Hardness: ≈ 63 HRM, as shown Figure S1g, Supporting Information). The dynamic friction coefficient, thermophysical properties, and hardening behavior of the micro–nanocomposite have been significantly improved by employing micro–nano-

composite, showed its superiority compared to the data of conventional triboelectric materials, such as PTFE, FEP, PDMS, and PI polymers. The results indicated that the friction properties may meet the strict requirements of “brake pad industry” by wearing tests (Figure 1d; Figure S1e,f, Supporting Information) so that it is capable of being used as a key supporting part such as automobile's brake pads. Subsequently, the composite structure of heTENG was fabricated based on the wear-resistant composite, as illustrated in Figure 1a and Figure S2 (Supporting Information), in which the heTENG was composed of freestanding mode TENG (heTENG-I) and single electrode mode TENG (heTENG-II). The heTENG-I is assembled by copper electrode layer, PTFE film, PTFE circular grid frame, filled with Al balls, Q235 steel as backplane, and the counter electrode, in which it is mainly to be used for harvesting vibration energy and self-powered sensing. The heTENG-II fabricated by the wear-resistant micro–nanocomposite serves as the triboelectric layer and copper film serves as the electrode connected with the external load, in which it is to be used for harvesting sliding energy in harsh environment (linear motion, circular motion).

2.1. The Working Mechanism of heTENG

The heTENG is schematically illustrated in **Figure 2a**, the basic unit consists of a freestanding mode heTENG-I and a single electrode mode heTENG-II (Figure 2b). The working mechanism and numerically calculated electrical potentials distribution of the heTENG are presented in Figure 2b–e. Based on the triboelectric and electrostatic conduction effects, an alternating charge flow can be produced in an external load to form a sustainable power source. The device of heTENG-I works basically in accordance with the freestanding mode.^[26] When the fabricated device is placed in working environment, the Al balls on the PTFE frame directly collide up and down between the two PTFE films as driven by vibration (Figure 2b). When the Al balls contact the bottom PTFE film (step 1), it would form the negative electrostatic charges on the surface of the PTFE films due to the high electron negativity of PTFE,^[27,28] the positive charges on the surface of the Cu electrodes, and Al balls. When the pellets move upward, the negative charges will flow from bottom Q235 steel electrode to the top Cu electrode to achieve a new electrostatic balance, forming a current under the short-circuit condition (step 2). After the Al balls collide with top PTFE film and move downward (step 3), the negative charges in the top electrode will flow to the bottom electrode to return to the original electrostatic status.^[29] As a result, it would form a reverse current in the short-circuit condition (step 4). This procedure forms the fundamental processes of converting vibration energy into electricity.

The working mechanism of the heTENG-II is based on the single model^[27,30] in which the electrode on the bottom part of the heTENG-II is grounded. It includes four typical steps, as shown in Figure 2d. At the initial step 1, both sides of triboelectric material/Cu electrode and top metal object (such as car's hub) are in separate and there is no current flow or electrical potentials. When the bottom composite triboelectric material/Cu electrode approaches the top metal object (step 2) and contacts (step 3), the resulted charge separation will induce negative potential on the Cu electrode, negative charges will be driven from grounded

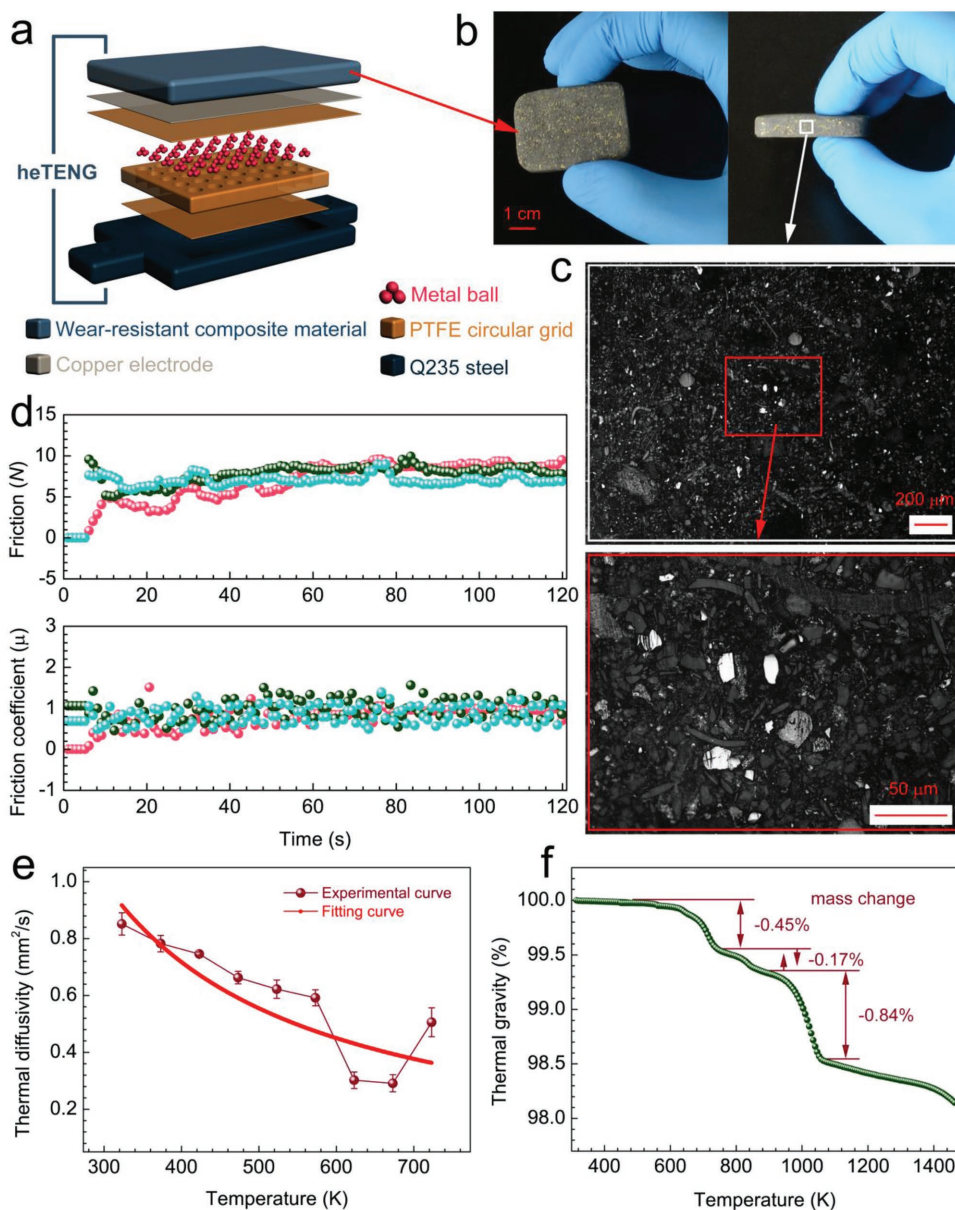


Figure 1. The structure and performance of harsh-environmental triboelectric nanogenerator (heTENG). a) Schematic diagram showing the structure of heTENG. b) Digital image of the wear-resistant composite material and c) its optical images. d) Friction properties of the wear-resistant composite material. e) Thermophysical properties of the wear-resistant composite material. f) Thermogravimetry of the wear-resistant composite material.

electrode to the Cu electrode. Sequentially, go through step 3, step 4 to step 1 that will form the reverse current. Since the size of the heTENG-II is finite, an approaching or departing of the top metal object from the bottom one would change the local electrical field distribution, so that there are electron exchanges between the bottom Cu electrode and the ground to maintain the potential change of the electrode. To theoretically predict the distribution of the electrical potential between the Cu electrode and Q235 steel electrode, COMSOL software that employs the finite element method was implemented (Figure 2c,e). At the starting point, the calculated electrical potential difference between the two electrodes is zero (step 1). Then, a potential is generated to keep the charge balance according to the simulation

(step 2, step 3, and step 4). Based on the converting process, the generated current can essentially be described by the second terms (polarization charge) of the corresponding displacement current in the Maxwell equation as proposed by Wang (Equations (S1) and (S2)).^[26,31]

2.2. The Electrical Output Performances of the heTENG

The use of the heTENG is extensive, e.g., it can be applied to serve as brake pads in machines and vehicles that enables both harvesting sliding energy (linear motion, circular motion), vibration energy (vibrational angle is $\alpha = 0^\circ, 45^\circ, \text{ and } 90^\circ$),

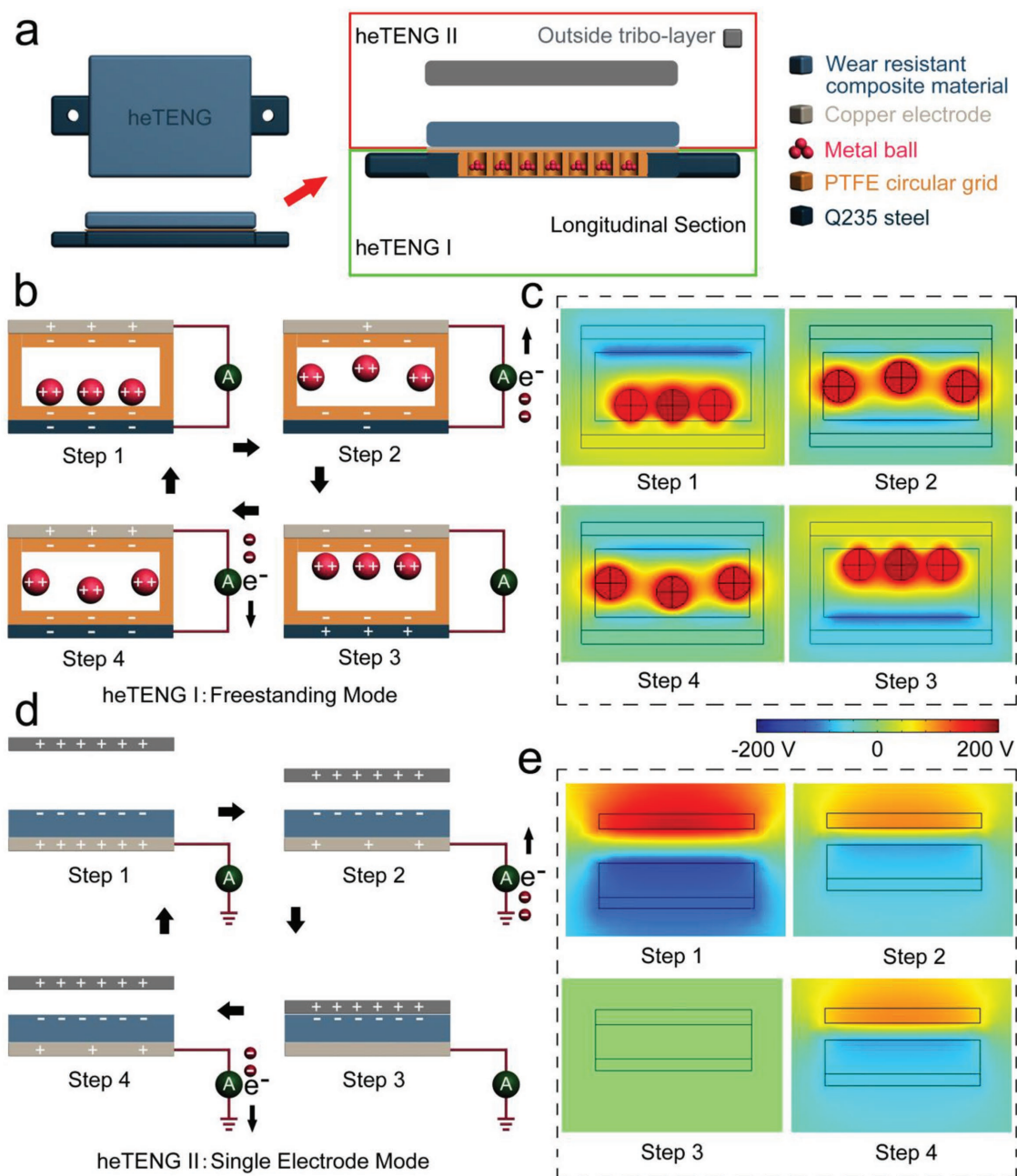


Figure 2. Working process and principles of heTENG. a) Diagrammatic drawing showing the structure of heTENG. b) Schematic diagram showing the working process and principles of heTENG-I freestanding mode. c) The numerically calculated electrical potentials distribution of heTENG-I freestanding mode. d) Schematic diagram showing the working process and principles of heTENG-II single electrode mode. e) The numerically calculated electrical potentials distribution of heTENG-II single electrode mode.

and self-powered vibration sensing from the operational environment, as indicated in **Figure 3a,b**. To measure the electrical output of heTENG, we prepared a device with the size of 4 cm × 3 cm × 1.2 cm (Figure S1, Supporting Information) in experiments and trigger it by a linear motor for all following tests. The frequency of the relative motion between the heTENG and the metal object is set at 2 Hz. At this point, the peak voltage (V_{oc}) is around 14.5 V at the open-circuit conditions, as shown in Figure 3c (left). Under the short-circuit conditions,

the current (I_{sc}) was measured with a peak value of $\approx 2.7 \mu A$ (Figure 3d, left). Figure 3e (left) shows the transfer charge (Q_{sc}) of ≈ 5.7 nC in each cycle. The results demonstrated that only the heTENG-I works and harvests the vibration energy when there is no contact between them. On the other hand, when the contact–separation process occur that the heTENG and metal object are not slipping relative to each other, based on the wear-resistant composite’s heTENG-II was taken part in the energy harvesting and played an important role in improving

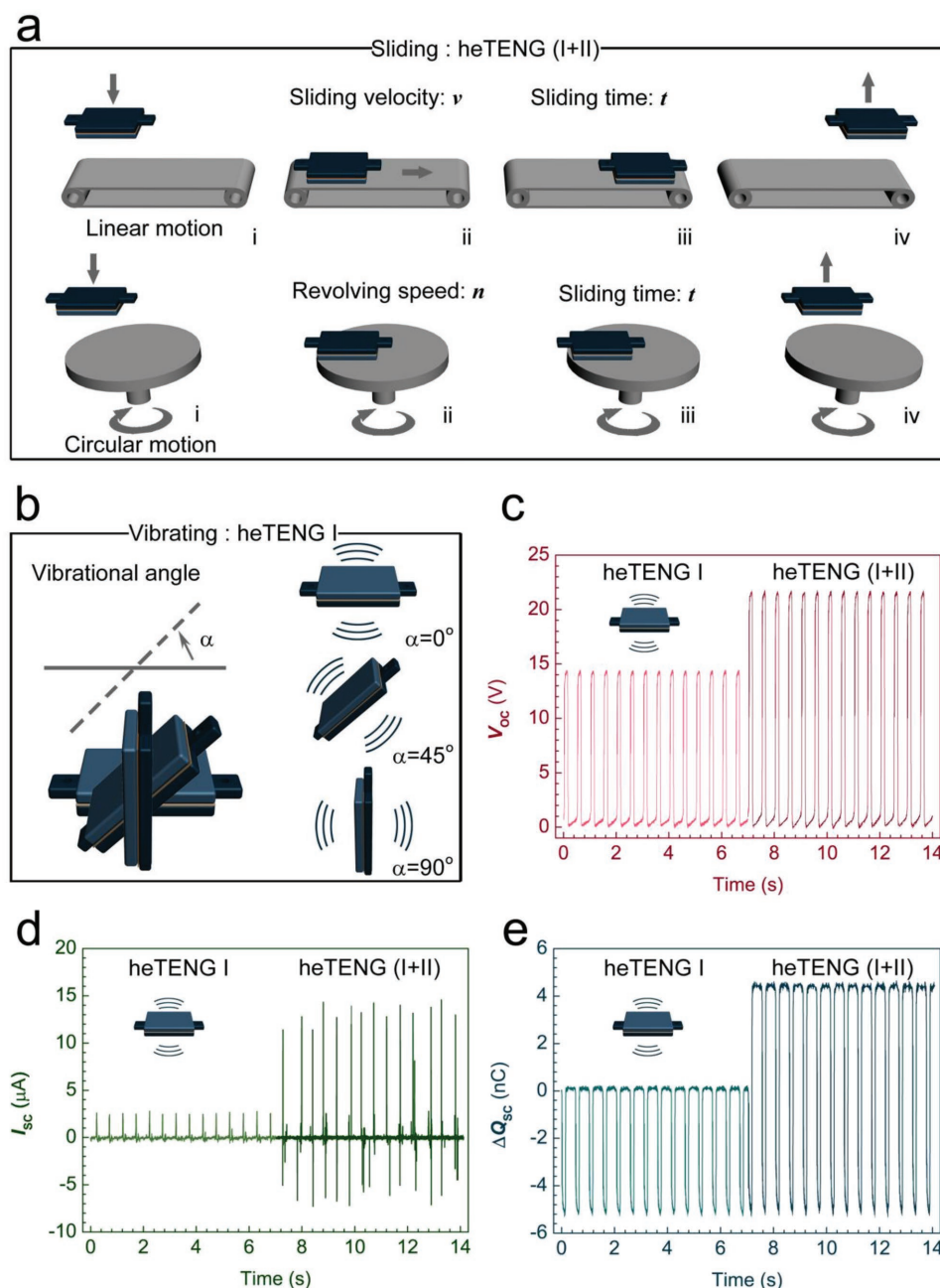


Figure 3. The workplace scenario and electrical output performances of heTENG. a,b) Diagrammatic drawings showing the workplace scenario of heTENG. c) Output open-circuit voltage of heTENG. d) Output short-circuit current of heTENG. e) Transferred charges quantity of heTENG.

output performances. The results showed that the output of the heTENG increased up to 22 V, 21 μA , and 10.5 nC at a frequency of 2 Hz, respectively (Figure 3c–e, right), indicating that the heTENG-II based on the wear-resistant composite has positive effect on the heTENG's output. It proves that the wear-resistant composite is efficient as a triboelectric material that can be used to harvest energy in harsh environment.

Obviously, the effective contact area and the structure of triboelectric layers are main factors that influence the heTENG's output performance, according to previous researches. A series of parameters that affect the output performance were adjusted

by optimized the design, and corresponding V_{oc} , I_{sc} , and Q_{sc} were measured with the same size of heTENG. The structure and parameters (r , R , and h) of heTENG were shown **Figure 4a**. The V_{oc} , I_{sc} , and Q_{sc} increase nonlinearly with the increase of vibrational frequency with a range of 1–40 Hz, as shown in **Figure 4b** and **Figure S2** (Supporting Information). This is because the output performance depends on the Al balls' collision probability between the bottom and the top PTFE films under noncontact mode motion. However, the output performance of the heTENG increased with the Al balls' fill number increasing first and then decreased. It reached its

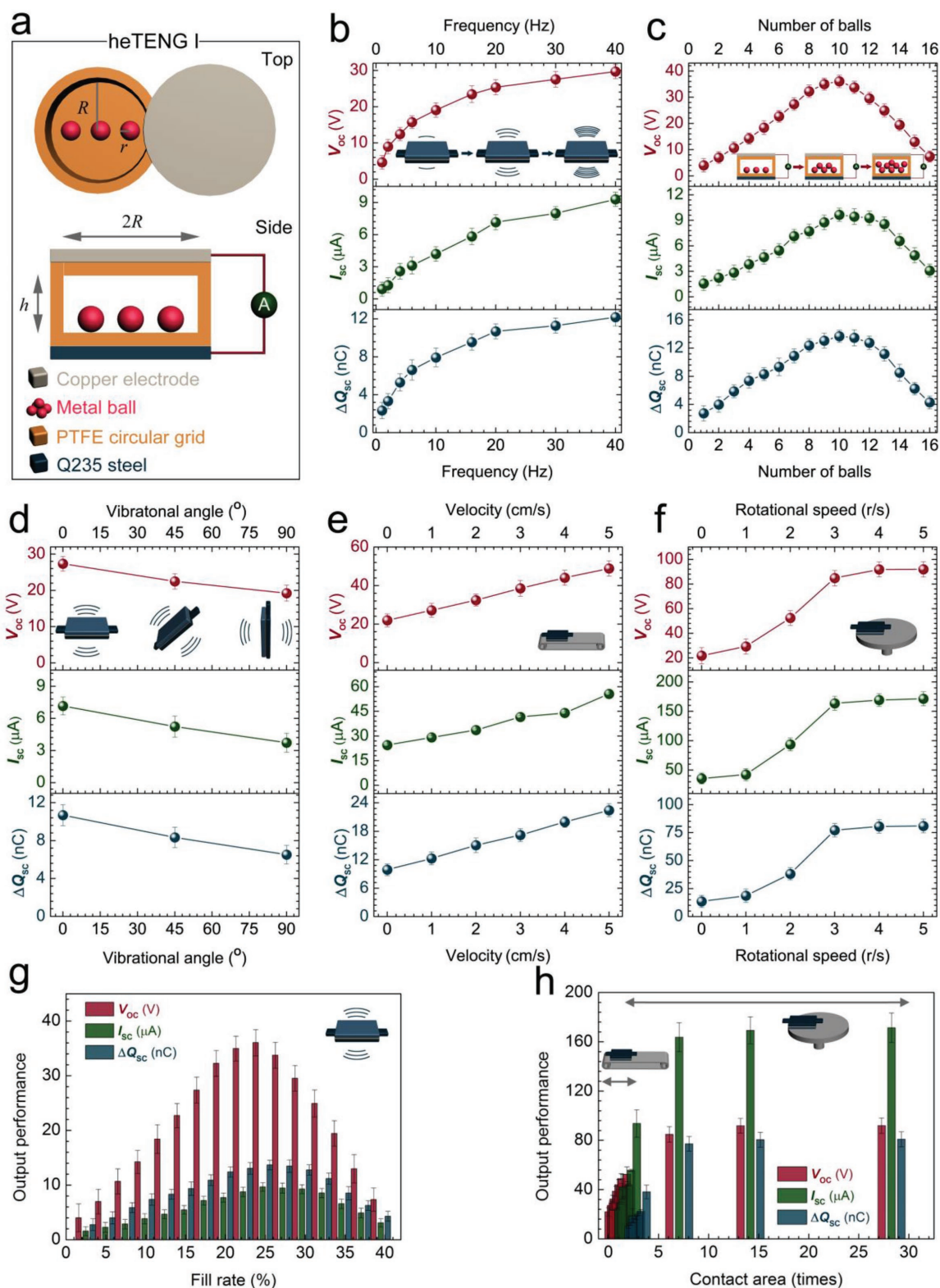


Figure 4. The influence of structure parameters on the electrical output performances of heTENG. a) Diagrammatic drawing showing the structure of heTENG-I. b) The influence of frequency on the electrical output performances of heTENG. c) The influence of number of balls on the electrical output performances of heTENG. d) The influence of vibrational angle on the electrical output performances of heTENG. e) The influence of velocity on the electrical output performances of heTENG. f) The influence of rotational speed on the electrical output performances of heTENG. g) The influence of fill rate on the electrical output performances of heTENG. h) The influence of contact area on the electrical output performances of heTENG.

maximum value when the number is about 10, as shown in Figure 4c and Figure S3 (Supporting Information). Provided that other conditions are invariant, the output performance of heTENG decreased with the vibrational angle ranging from 0°, 45°, and 90° (Figure 4d; Figure S4, Supporting Information). The reasons for these results, the collision probability decreased lead to that the decrease of contact area dramatically was the main reason. The relative sliding between the heTENG and the metal object under contact–separation mode was achieved and the output performance of heTENG was enhanced significantly with the increase of linear velocity v (cm s^{-1}) and rotational speed n (r s^{-1}), as shown in Figure 4e,f (Figures S5 and S6, Supporting Information), for improving the contact area of triboelectric layer at per unit time. Meanwhile, the fill rate of Al balls and equivalent contact area at relative sliding (a multiple of heTENG's triboelectric layer area) to influence that the output performance were shown in Figure 4g,h. Based on the same principle, the larger the effective contact area is, the more electrostatic charges generates. This can be explained by Equations (S1) and (S2) by Wang, as that the output majorly depends on the function of the gap distance $z(t)$ between the two dielectrics. The results indicate that the wear-resistant heTENG could efficiently harvest energy from various kinds of vibration and sliding motion in harsh environment to power electronics and various applications.

2.3. The Self-Powered Smart Braking Device Based on the heTENG

On the basis of the strong advantages of heTENG was demonstrated above, we develop an automobile's SP-SB device that can be used for automatic early-warning when there is a need to replace the brake pads without any professional engineering technique personnel intervention in the field, the typical application scenarios and structure of the SP-SB device were shown in Figure 5a,b. The digital photograph and equivalent circuits of the SP-SB device are shown in Figure 5c,d, respectively. It comprised of a heTENG device, a diode-bridge (rectify the alternating output signals), a 1 μF capacitor (accumulation charge), a switch, and a wireless transmitter and receiver integrated circuit board. The relationship between the performances of SP-SB device and automobile's engine speed from 500 to 4000 r/min is shown in Figure 5e. The V_{oc} , I_{sc} , and Q_{sc} increase linearly with the increase of engine speed, this is because the output performance depends on the sliding area of triboelectric layer. The triboelectric layer was appeared thin wear at high engine speeds that equivalent to obviously increased contact area in a short period of contact–separation (about 1 s). So, but more importantly, the maximum surface charge density limit of the triboelectric material was broken through that because a brand-new triboelectric layer formed gradually on the triboelectric material with the friction process.^[32,33] The procedure of charging based on these circuits is presented in Figure 5f. The results showed the relationship between the charging voltage and number of times (contact–separation) under engine speed of 2000 r min^{-1} . The SP-SB device emits a signal when the capacitor reaches a predetermined charging voltage (3 or 4.5 V), in which the threshold voltage can make an adjustment based on different integrated circuit.

For another, the two metal electrodes was prefabricated in the heTENG' triboelectric layer, as shown in Figure 5g. When the maximum limit is reached to the triboelectric material wear extent, the two metal electrodes will is leaking in this moment, which causes a short circuit and can result in voltage sags when they contact the external metal object (for example, automobile hub). This is because of the heTENG-II stopped working altogether at short circuit, only the heTENG-I is still running normally, so that, which can alert to us the repair replacement of brake pad immediately. For instance, the output voltage of the heTENG was dropped to the limited operating voltage (V_{LO}) of 14.5 and 22.5 V under engine speed of 0 and 2000 r min^{-1} conditions (the yellow lines in Figure 5h), this indicate it is time to replaced the triboelectric layer (brake pad). This avoids the security exposure entirely, it is good news for the non-professional and particularly for autonomous vehicles.

2.4. The DSEW Sensor Network Based on the SP-SB Device

Vibration is one of the most common mechanical motions that ubiquitously available in driving of vehicle. The seven degree of freedom (DOF) model of automobile vibration was established,^[34,35] as shown in Figure 6a. Automobile vibration has something to do with many factors of which load and tire pressure are the major, at the same time are the main factors of influencing running safety. The vibration results from them simulated and analyzed by the MATLAB software, the amplitude–frequency curve of automobile vibration was shown in Figure 6b. By adjusting the parameters in the DOF model, the results of simulation confirmed that the influencing factors of the overweight, eccentric load, and tire pressure were not only the ride comfortableness, but also automobile's ride stability and safety, as shown in Figure 6c and Figures S7–S10 (Supporting Information). Based on SP-SB device's sensitivity, a sensor network was established by using four SP-SB devices for vehicle's DSEW system was shown in Figure 6d. First, the relationship between the voltage of sensor network and automobile's load form 60 to 540 kg was shown in Figure 6e, the voltage increased with the increased the load weight, but the change rule is a nonlinear curve. When the load reach or almost reach 360 kg (amount to the weight of six people, including a driver), the output voltage has a remarkable increasing with linear increasing trend. At this point, the vibration of automobile was enhanced remarkably and the voltage of 210V is an indicator of overweight, while a reading of nearly 30 V or more indicates dangerously overloaded. Second, the relationship between eccentric load state (I, II, III) and voltage of the sensor network can be used for eccentric load monitoring, as shown in Figure 6f and Figure S11 (Supporting Information). Taking example for two people load, the position of the people in the automobile are as follows: FL-FR (state I), FL-RR (state II), and FL-RL (state III), the load state was shown by the output voltage distribution of sensor network. Finally, the relationship between tire pressure (state 1, state 2, and state 3) and output voltage of sensor network were shown in Figure 6g. The results showed that the state of tire pressure were as follows: one for the normal state (state 1), the front right tire was lowed pressure (state 2), and the right rear tire was as lowed pressure (state 3). So that, a novel type of

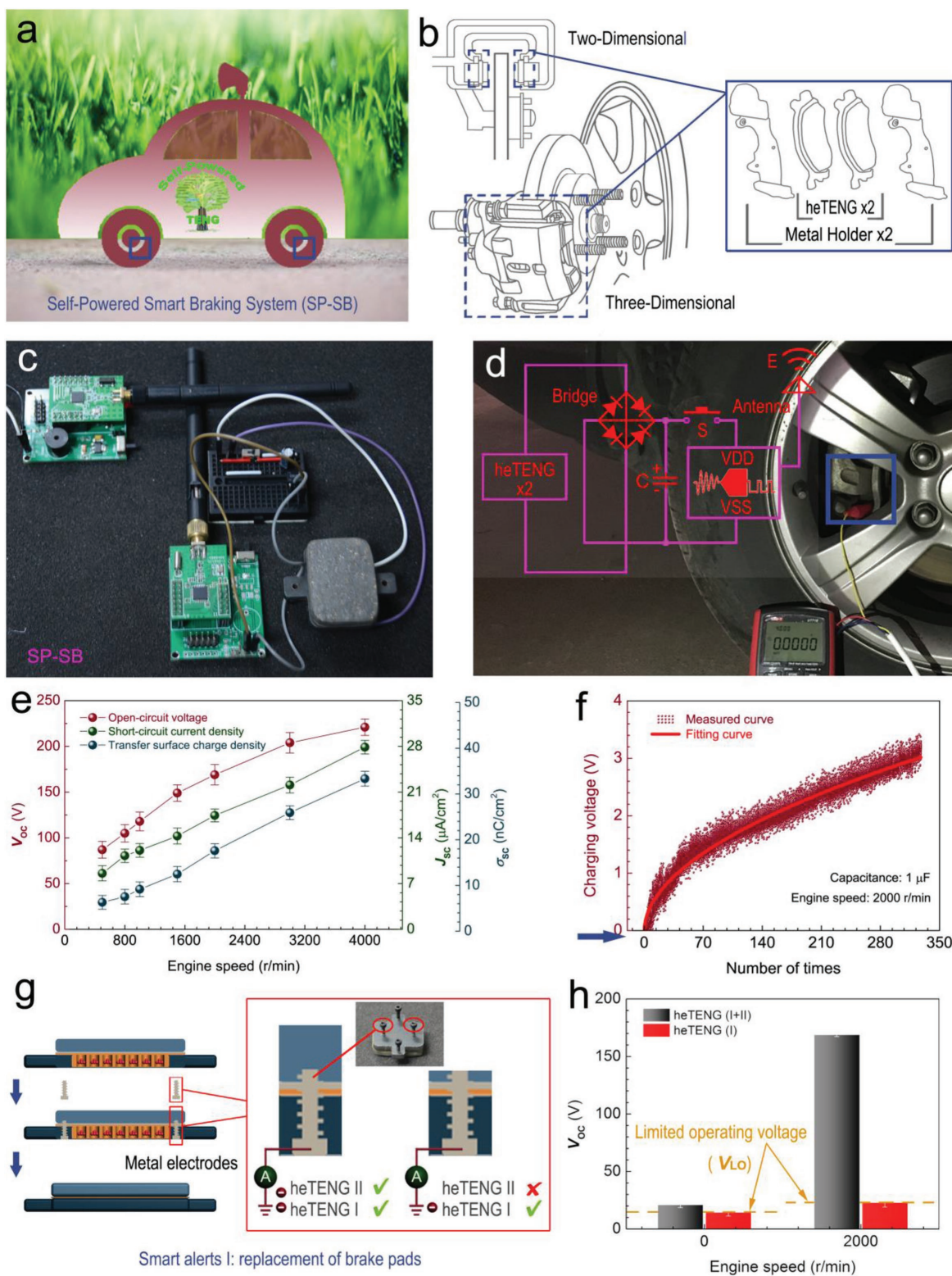


Figure 5. Mechanical energy harvesting by heTENG as a self-powered smart braking (SP-SB) device used in autonomous car. a) Application of the SP-SB used for autonomous car. b) Diagrammatic drawing showing the engineering structure of the SP-SB. c) Digital photograph showing the assembly part of the SP-SB. d) Digital photograph of the SP-SB used in autonomous car and its circuit diagram. e) Output performances of heTENG used for autonomous car. f) The voltage–number of times relationship at load capacitances of 1 μF . g) Diagrammatic drawing showing the engineering structure of the SP-SB as smart alerts I: replacement of brake pads. h) Limited operating voltage of the SP-SB at different engine speed as smart alerts I: replacement of brake pads.

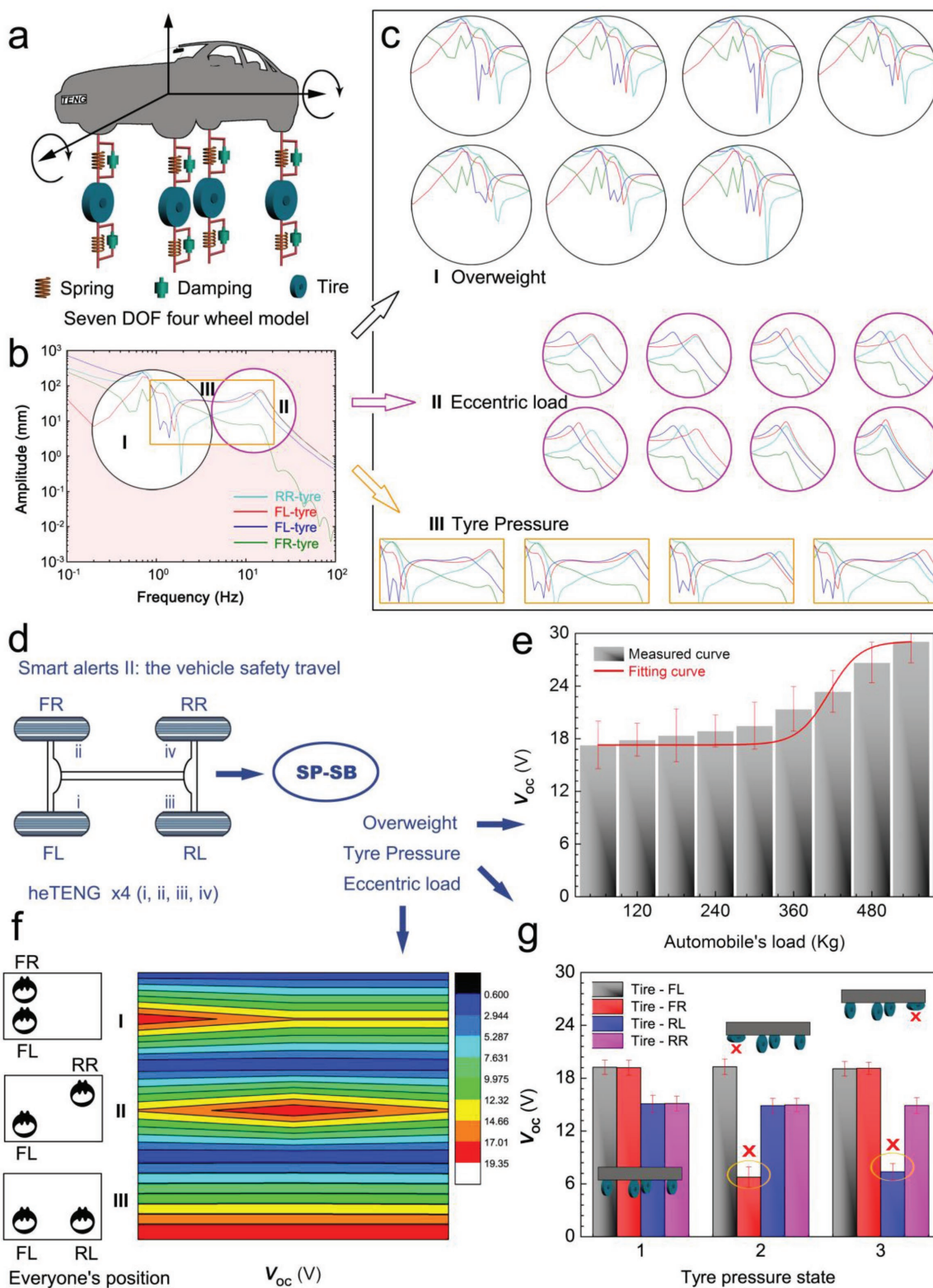


Figure 6. Seven degree of freedom (DOF) model of car and its DSEW sensor network based on the SP-SB device. a) Seven DOF four-wheel model of car. b) The relationship between frequency and amplitude of seven DOF model by MATLAB simulation. c) The relationship between frequency and amplitude of seven DOF model at different external conditions. d) Application of the SP-SB based on four heTENGS used for smart alerts II: the vehicle safety travel. e) The relationship between automobile's load and voltage of the SP-SB used for overweight monitoring. f) The relationship between eccentric load state (I, II, III) and voltage of the SP-SB used for eccentric load monitoring. g) The relationship between tire pressure state (1, 2, 3) and the voltage of the SP-SB used for tire pressure monitoring.

vibrational sensor network is constructed for safety monitoring of vehicle with combinations of four SP-SB device, that can not only acquire vibrational voltage signal of the driving status but also supply the DSEW and take proper action in real time, such as overweight, eccentric load, and tire pressure.

3. Conclusions

In summary, we designed a wear-resistant material by hybridizing micro–nanocomposite and its application as a single electrode for a TENG's triboelectric layer was introduced. It is suitable for being used in harsh environment to harvest sliding energy. The results showed that the micro–nanocomposite had a good wear resistance that the mean dynamic friction coefficient of $\approx 0.69 \mu\text{m}$ at low-friction of about 8.1 N and room temperature (Figure 1d; Figure S1e, Supporting Information), and it had excellent high-temperature tolerance (temperature range of -30 to 550°C), the wear-resisting ability (Figure S1f, Supporting Information), and high hardness (Rockwell Hardness: ≈ 63 HRM, as shown Figure S1g, Supporting Information), making it capable of being used as a key supporting part such as automobile's brake pads. Combining freestanding-mode TENG, the complex heTENG can both harvest slide/vibration energy and self-powered sense the vibration signal. A high output performance of 221 V, $27.9 \mu\text{A cm}^{-2}$, and $33.4 \mu\text{C cm}^{-2}$ under high engine speed of 4000 r min^{-1} and a frequency around 1 Hz were produced. Furthermore, an SP-SB system based on the heTENG was developed successfully which can automatically provide exact early-warning when the brake pads need being replaced. Simultaneously, a sensor network was fabricated by using four SP-SB devices for automobile's DSEW system, which may provide an early-warning such as overweight, eccentric load, and tires' pressure monitoring. Our work not only shows a new strategy to enhance the wear-resistant performance of triboelectric materials to make it applicable for harsh environment, but also provides new opportunities for sliding energy harvesting and multifunctional self-powered sensing and potential applications in autonomous vehicle and industrial brakes.

4. Experimental Section

In this experiment, the triboelectric material's preparation process, morphology, and microstructure were shown in Figure 1 and Figure S1 (Supporting Information). The wear-resistant of triboelectric materials were prepared by hybridizing micro–nanocomposite, Figure S1a of the Supporting Information shows the fabrication process in detail. In this experiment, the micro–nanocomposite powders were prepared by ball-milling method that contained a thermosetting binder resin ($\approx 8.5 \text{ wt}\%$), reinforcing micro–nanofiber ($\approx 26.4 \text{ wt}\%$), friction performance regulator ($\approx 34 \text{ wt}\%$), complex filler ($\approx 20.7 \text{ wt}\%$), triboelectric modifier ($\approx 9.5 \text{ wt}\%$), and other materials (bal.). Then the mixture of micro- and nanopowders is put into the mould of design, hot press molding, heat treatment, postprocessing (polished and cut) with dimensions of $4 \text{ cm} \times 3 \text{ cm} \times 0.7 \text{ mm}$. The process parameters of preparing triboelectric material were followed: the milling time of 10 min, hot-pressing temperature of 165°C , pressure of 20 MPa, dwelling time of 7 min, heat treatment temperature of 200°C , and time is above 8 h.

The wear-resistant properties of the composite were characterized by high temperature friction and wear tester, the experiment results were shown in Figure 1d and Figure S1e,f (Supporting Information).

Furthermore, the effects of wear time on friction properties of the composite materials have been investigated by the 24 h durability test (Figure S1e, Supporting Information). Simultaneously, the relationship between wear rate (ω , $10^{-7} \text{ cm}^3 (\text{N m})^{-1}$) and work temperature (K) was investigated, as shown in Figure S1f of the Supporting Information. The hardness of the composite was measured using automatic Rockwell Hardness tester (Figure S1g, Supporting Information). The thermophysical properties of the composite were characterized by laser flash apparatus (NETZSCH, LFA 427) and thermogravimetry (NETZSCH, DSC/TG 449 F3), as shown in Figure 1e,f. The dynamic friction coefficient, thermophysical properties, and hardening behavior of the micro–nanocomposite were determined and analyzed for revealing fundamental friction performance compared to conventional triboelectric materials. Subsequently, the wear-resistant composite was utilized to construct a heTENG, where one part comprises of triboelectric layer, Cu electrode, metal balls, PTFE circular grid as the frame, PTFE film, and Q235 steel (Figure 1a). The heTENG was composed of freestanding mode heTENG-I and single electrode mode heTENG-II. The heTENG-I is assembled by copper film electrode, PTFE film, PTFE circular grid as the frame, Q235 steel support and filled with Al balls, and the Q235 steel as the counter electrode, which are also utilized to contact with the PTFE films. The heTENG-II is fabricated by that the wear-resistant micro–nanocomposite serves as the triboelectric layer, copper film serves as the electrode connected with the external load. The electrical output signals of the heTENGs were measured by a Keithley voltage preamplifier and a Data Acquisition Card. The software platform is constructed based on LabVIEW, which can realize real-time data acquisition control and analysis. The potential distribution in the TENG was calculated from a finite-element simulation using COMSOL software. The vibration results from the simulated and analyzed by the MATLAB software, the amplitude–frequency curve of automobile vibration was shown in Figure 6b,c and Figures S8–S10 (Supporting Information). The output of the SP-SB system and sensor network was tested at different engine speed (r min^{-1}) by the platform of four-wheel positioning detection (Figures 5 and 6).

Supporting Information

Supporting Information is available from the Wiley Online Library or from the author.

Acknowledgements

J.W., B.C., and W.T. contributed equally to this work. This study was supported by the "Thousands Talents" program for pioneer researcher and his innovation team, China, thanks for the support from the National Natural Science Foundation of China (Grant Nos. 51462026, 51672136, 61405131, 51432005, 5151101243, 51561145021, 51702018, and 11704032), the National Key R&D Project from Minister of Science and Technology (2016YFA0202704), Beijing Municipal Science & Technology Commission (Y3993113DF and Z171100000317001).

Conflict of Interest

The authors declare no conflict of interest.

Keywords

self-powered smart braking, sliding energy harvesting, triboelectric nanogenerator, wear-resistant composite

Received: June 18, 2018

Revised: July 25, 2018

Published online:

- [1] Z. L. Wang, J. Song, *Science* **2006**, 312, 242.
- [2] F. R. Fan, Z. Q. Tian, Z. L. Wang, *Nano Energy* **2012**, 1, 328.
- [3] Z. L. Wang, *ACS Nano* **2013**, 7, 9533.
- [4] J. Chen, Z. L. Wang, *Joule* **2017**, 1, 480.
- [5] G. Zhu, J. Chen, T. J. Zhang, Q. S. Jing, Z. L. Wang, *Nat. Commun.* **2014**, 5, 3426.
- [6] S. W. Chen, C. Z. Gao, W. Tang, H. Zhu, Y. Han, Q. W. Jiang, T. Li, X. Cao, Z. L. Wang, *Nano Energy* **2014**, 14, 217.
- [7] J. Wang, S. Li, F. Yi, Y. Zi, J. Lin, X. Wang, Y. Xu, Z. L. Wang, *Nat. Commun.* **2016**, 7, 12744.
- [8] F. Yi, X. Wang, S. Niu, S. Li, Y. Yin, K. Dai, G. Zhang, L. Lin, Z. Wen, H. Guo, J. Wang, M. H. Yeh, Y. Zi, Q. Liao, Z. You, Y. Zhang, Z. L. Wang, *Sci. Adv.* **2016**, 2, e1501624.
- [9] X. F. Wang, S. M. Niu, Y. J. Yin, F. Yi, Z. You, Z. L. Wang, *Adv. Energy Mater.* **2015**, 5, 1501467.
- [10] Z. L. Wang, *Nature* **2017**, 542, 159.
- [11] Y. Xi, H. Y. Guo, Y. L. Zi, X. G. Li, J. Wang, J. N. Deng, S. M. Li, C. G. Hu, X. Cao, Z. L. Wang, *Adv. Energy Mater.* **2017**, 7, 1602397.
- [12] J. Chen, Y. Huang, N. Zhang, H. Zou, R. Liu, C. Tao, X. Fan, Z. L. Wang, *Nat. Energy* **2016**, 1, 16138.
- [13] W. Tang, T. Jiang, F. R. Fan, A. F. Yu, C. Zhang, X. Cao, Z. L. Wang, *Adv. Funct. Mater.* **2015**, 1, 1501331.
- [14] W. Tang, B. Meng, H. X. Zhang, *Nano Energy* **2013**, 2, 1164.
- [15] L. Jin, S. Ma, W. Deng, C. Yan, T. Yang, X. Chu, G. Tian, D. Xiong, J. Lu, W. Yang, *Nano Energy* **2018**, 50, 632.
- [16] B. Chen, W. Tang, C. Zhang, L. Xu, L. Zhu, L. Yang, C. He, J. Chen, L. Liu, T. Zhou, Z. L. Wang, *Nano Res.* **2018**, 11, 3096.
- [17] C. He, C. Han, G. Gu, T. Jiang, B. Chen, Z. Gao, Z. L. Wang, *Adv. Energy Mater.* **2017**, 7, 1700644.
- [18] C. H. Yang, B. Chen, J. Zhou, Y. M. Chen, Z. Suo, *Adv. Mater.* **2016**, 28, 4480.
- [19] X. Chen, X. Pu, T. Jiang, A. Yu, L. Xu, Z. L. Wang, *Adv. Funct. Mater.* **2016**, 27, 1603788.
- [20] B. Chen, W. Tang, C. He, C. Deng, L. Yang, L. Zhu, J. Chen, J. Shao, L. Liu, Z. L. Wang, *Mater. Today* **2018**, 21, 88.
- [21] J. Wang, S. Li, F. Yi, Y. Zi, J. Lin, X. Wang, Y. Xu, Z. L. Wang, *Nat. Commun.* **2016**, 7, 12744.
- [22] C. B. Han, C. Zhang, X. H. Li, L. Zhang, T. Zhou, W. Hu, Z. L. Wang, *Nano Energy* **2014**, 9, 325.
- [23] B. Chen, W. Tang, T. Jiang, L. Zhu, X. Chen, C. He, L. Xu, H. Guo, P. Lin, D. Li, J. Shao, Z. L. Wang, *Nano Energy* **2018**, 45, 380.
- [24] Z. L. Wang, J. Chen, L. Lin, *Energy Environ. Sci.* **2015**, 8, 2250.
- [25] B. Chen, W. Tang, C. He, T. Jiang, L. Xu, L. Zhu, G. Gu, J. Chen, J. Shao, J. Luo, Z. L. Wang, *Adv. Mater. Technol.* **2018**, 3, 1700229.
- [26] Z. L. Wang, *Mater. Today* **2017**, 20, 74.
- [27] Z. H. Lin, G. Cheng, S. Lee, K. C. Pradel, Z. L. Wang, *Adv. Mater.* **2014**, 26, 4690.
- [28] Y. Xi, J. Wang, Y. L. Zi, X. G. Li, C. B. Han, X. Cao, C. G. Hu, Z. L. Wang, *Nano Energy* **2017**, 38, 101.
- [29] C. He, W. Zhu, G. Gu, T. Jiang, L. Xu, B. Chen, C. Han, D. Li, Z. L. Wang, *Nano Res.* **2017**, 11, 1157.
- [30] X. Y. Wei, G. Zhu, Z. L. Wang, *Nano Energy* **2014**, 10, 83.
- [31] Z. L. Wang, T. Jiang, L. Xu, *Nano Energy* **2017**, 39, 9.
- [32] S. Wang, Y. Xie, S. Niu, L. Lin, C. Liu, Y. S. Zhou, Z. L. Wang, *Adv. Mater.* **2014**, 26, 6720.
- [33] T. Zhou, L. M. Zhang, F. Xue, W. Tang, C. Zhang, Z. L. Wang, *Nano Res.* **2016**, 10, 1007.
- [34] S. M. Babcock, R. V. Dubey, J. A. Euler, R. L. Glassell, R. L. Kress, *Geophys. Res. Lett.* **1988**, 35, 344.
- [35] K. Kreutz-Delgado, M. Long, H. Seraji, *Int. J. Rob. Res.* **1992**, 11, 469.